J. Fluid Mech. (1989), *vol.* 209, *pp.* 617–637
Printed in Great Britain

Growth and translation of a liquid–vapour compound drop in a second liquid. Part 1. Fluid mechanics

By S. T. VUONG AND S. S. SADHAL
Department of Mechanical Engineering, University of Southern California, Los Angeles, CA 90089-1453, USA

(Received 21 March 1989)

The fluid dynamics associated with a compound drop consisting of a vapour bubble, partly surrounded by its own liquid in another immiscible liquid is considered. The fluid motion is analysed in the limit of Stokes flow and at the same time the surface tension forces are considered to be large enough to allow the interfaces to have uniform curvature. The flow field consists of translation and growth that can arise from change of phase.

An exact analytical solution for the axisymmetric flow field is obtained. The important results of physical interest are the drag force and the flow behaviour. In the case without growth, the drag force lies between the bubble and the solid-sphere limits for a sphere of the same volume as the total liquid and vapour dispersed phase. The maximum drag force is observed when the liquid and vapour volumes are nearly the same. This is the effect of weak circulation due to the smaller available space as compared with a spherical drop. With growth this effect appears to be enhanced. The flow streamlines exhibit secondary vortices in the dispersed phase when there is growth. The velocity field and the drag results here are applied to the heat transfer problem for the compound drop in Part 2 of this two-part series.

1. Introduction

The study of compound multiphase droplets has been of great interest in recent years because of its wide range of applications in many fields of engineering. We encounter these drops in processes such as direct-contact heat exchange, liquid-membrane technology and the melting of ice particles in the atmosphere. Chambers & Kopac (1937) and Kopac & Chambers (1937) studied the subject of compound drops in connection with the coalescence of living cells and oil drops. Their work was subsequently followed by other researchers. Li & Asher (1973) developed the idea of coating drops and bubbles with liquid membranes for application in separation processes such as artificial blood oxygenation. Compound drops are also formed when direct-contact heat exchange takes place with a change of phase. Generally, drops of one liquid are passed through another immiscible liquid and this results in an efficient exchange of heat between the two liquids. If, say, the dispersed phase undergoes a phase change so that both the liquid and the vapour coexist for some time, then we have a compound drop. There have been numerous theoretical as well as experimental studies in this area. For example, Sideman & Hirsch (1965); Sideman, Hirsch & Gat (1965); Sideman & Gat (1966); Mercier *et al.* (1974); Hayakawa & Shigeta (1974); Tochitana, Mori & Komotori (1977*a*) and Tochitana *et al.* (1977*b*) have experi-

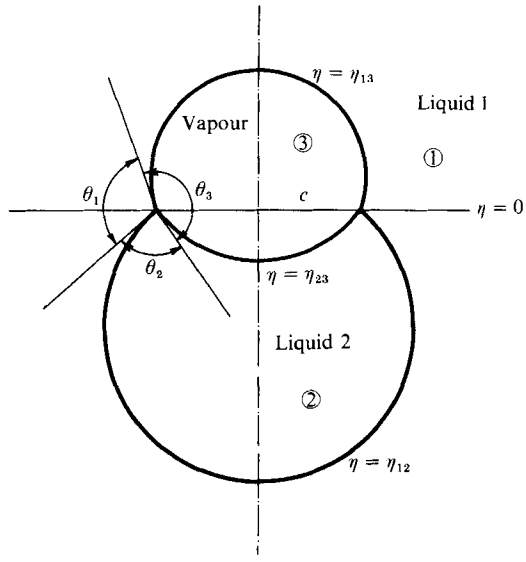

FIGURE 1. Configuration of a partially engulfed liquid–vapour compound drop.

mentally studied the fluid mechanics associated with such drops. However, little progress had been made in terms of the theoretical fluid mechanics until recently. The first thorough theoretical treatment of the static two-fluid compound drop configuration was carried out by Torza & Mason (1970) for studying three-phase interactions. Their analysis was restricted to static drops in the absence of gravity. Other theoretical studies of translation include that of Rushton & Davies (1983) who considered a compound drop consisting of concentric spheres. Recent theoretical studies on such fluid dynamics includes the analysis by Johnson & Sadhal (1983). They examined translating drops and bubbles partially coated with thin films by applying lubrication theory. They also gave an extensive review of the fluid mechanics of compound drops and bubbles (see Johnson & Sadhal 1985). The problem of the fluid mechanics of a compound drop consisting of a liquid drop or a gas bubble completely coated by another liquid, moving in a third immiscible fluid (2-singlet configuration) was investigated theoretically by Sadhal & Oğuz (1985). They also examined the stability of the dynamic equilibrium of the inner drop with respect to the whole compound drop. In a later development, Oğuz & Sadhal (1987) included the heat transfer for an evaporating or condensing drop.

The evaporation of a liquid drop into a vapour bubble can occur in three different configurations: non-engulfing, complete engulfing and partial engulfing (see Avedisian & Andres 1978). The prevalence of a particular equilibrium configuration can be best explained by the pure mechanics of balancing the surface tensions which depend largely on the types of fluids making up the system. This subject has been discussed by Torza & Mason (1970) extensively for a static compound drop and later elaborated upon by Johnson & Sadhal (1985) using the argument of minimum surface energy. Mori (1978) presented the same criteria for the three equilibrium configurations using experimental data.

The non-engulfing case of a compound drop is a situation in which the vapour phase is detached from the liquid phase and the two are in contact at one singular point. This is sometimes called bubble blowing as the vapour phase is blown away from the liquid phase. The complete engulfing is said to take place when the vapour

phase is entirely inside the liquid phase and the two can be concentric or eccentric to each other. While static drop configurations are governed purely by surface thermodynamics, the fluid motion can change the equilibrium criteria, especially for complete engulfing case.

The present development focuses on the 3-singlet configuration, that is, the case when each of the three fluids of the system is in contact with the other two. In particular, we are considering a vapour bubble partially engulfed by its own liquid (see figure 1). It consists of the liquid phase at the lower part of the compound drop and the vapour phase at the upper part. These types of droplets arise in the area of direct-contact heat transfer. In the present paper (Part 1) we are concerned purely with the fluid mechanics associated with the growth and translation of such drops. In Part 2 (Vuong & Sadhal 1989), the heat transfer is treated in detail.

2. Statement of problem

A schematic of a partially engulfed compound gas–liquid drop is depicted in figure 1. The drop consists of two parts: the liquid phase at the bottom and the vapour phase at the top. This equilibrium configuration is maintained by balancing the surface tensions at the interfaces assuming a static compound drop; this assumption is valid when the drop motion is slow. Initially, a drop of mostly liquid (dispersed phase) at uniform saturation temperature corresponding to the hydrostatic pressure of the fluid column is injected into the bottom of a different immiscible liquid (continuous phase) which is maintained at a slightly higher temperature than the drop. As the drop rises in the continuous phase under its own buoyancy force, it absorbs energy from the external fluid and evaporation takes place at the liquid–vapour interface. Part of the liquid phase of the drop is turned into vapour, resulting in a change of size and shape of the drop. In other words, the drop is growing in time. In the limit of the drop size being small (of the order of 1 mm) and a highly viscous continuous phase, the Reynolds number of the flow fields is small (less than the order of one) and Stokes flow can be assumed. The equations in this limit being linear allow a fully analytical solution. In a flow field dominated by viscous effects, the viscous diffusion affects the entire domain very quickly. Therefore we also neglect the time-dependent term and assume a quasi-steady state so that the steady-state solution of the flow field can be applied at any instant of time for the entire process while the drop is undergoing translation and growth. Because the Stokes equation is linear, it is convenient to decompose the flow field into two parts: one from the translation and the other from the growth. In the translation part, the rise of the drop due to the buoyancy creates an external flow field. Simple continuity at the liquid–liquid interfaces generates internal circulation. For the growth part, the process is more complicated, partly because of the complexity of the geometry and partly because of non-uniform normal velocities at the interfaces, which will be seen in the later sections. These two parts can actually be lumped together but we choose to separate them for the sake of clarity. Because of the creeping-flow assumption and because the growth process is slow, the surface tension forces are assumed to be large enough to keep the interfaces in a spherical shape and they will not be distorted by the variation of the normal stress. The Stokes equation is solved for both the external continuous phase and the liquid phase of the drop. The flow field in the vapour phase of the drop need not be solved because of insignificant viscosity. Also, the flow field is axisymmetric. Effects of natural convection, viscous dissipation, and compressibility are all neglected.

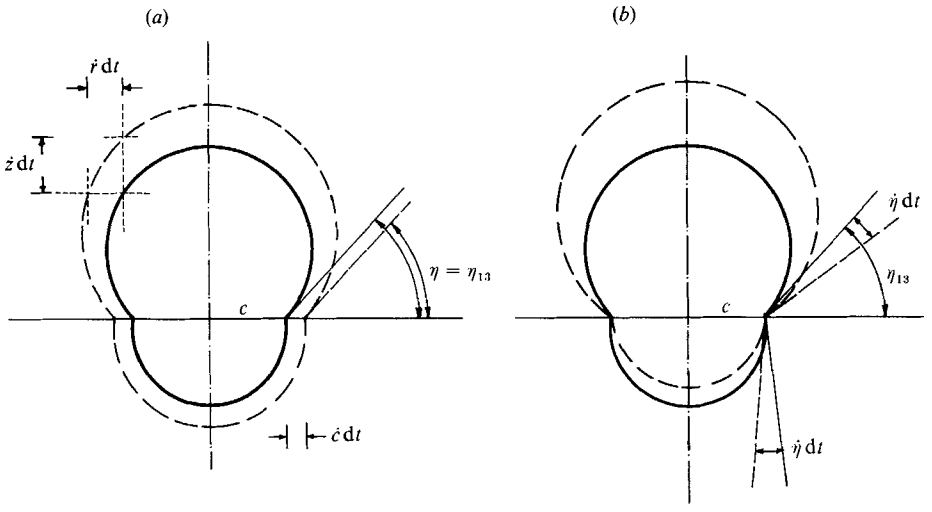

FIGURE 2. Infinitesimal shape changes arising from growth. (*a*) Growth due to increasing radius of contact circle; (*b*) growth due to angular motion about the contact circle.

The governing equations for fluid flow are as follows:

continuity $$\nabla \cdot \boldsymbol{u}_i = 0 \quad (i = 1, 2), \tag{1}$$

momentum $$\nabla p_i = \mu_i \nabla^2 \boldsymbol{u}_i \quad (i = 1, 2; \text{ no sum}), \tag{2}$$

where $i = 1, 2$ is used to denote the dispersed- and the continuous-phase liquids, respectively; the vapour phase is referred to as fluid 3; $\boldsymbol{u}_i$ are the velocities; p_i the pressures and μ_i the viscosities. The subscript i will, however, be dropped when referring to both liquids in general terms. The boundary and interface conditions are summarized below: (i) uniform free-stream velocity U_∞ at infinity; (ii) prescribed non-uniform radial velocities at all three interfaces due to growth; (iii) continuity of tangential velocity at the liquid–liquid interface 1–2; (iv) continuity of shear stress at the liquid–liquid interface 1–2; (v) zero shear stress at the two liquid–vapour interfaces 1–3 and 2–3.

The uniform free-stream velocity is not a constant but a variable of time because the configuration of the drop is changing as it grows. Since the drop is translating slowly and the rate of change is small, we ignore the transient term associated with the rate of change of the velocity, so that the terminal velocity at any instant can be determined by balancing the buoyancy force and the drag force. The growth velocities at the interfaces are a little peculiar; they include contributions of $\dot{\eta}$, which is the angular velocity of the interfaces about the contact circle and $\dot{c}$, which is the velocity of the contact circle (see figure 2). The velocities $\dot{\eta}$ are the same at all three interfaces so as to maintain the same contact angles, as will be seen later. The two different boundary velocities $\dot{c}$ and $\dot{\eta}$ cannot vary independently but have to satisfy a constraint that the volume of the liquid phase of the drop is instantaneously constant because of conservation of total mass. This will also be discussed in the section on the solution for the growth of the drop. Since the growth arises mainly from the change of phase, it depends on the evaporation rate, which is governed by the heat transfer aspects of the system. In this paper the growth rate will be prescribed arbitrarily. The detailed treatment of the heat transfer is given in Part 2.

3. Solution

The set of equations (1) and (2) can be solved for the velocity and pressure distribution. We use the alternative stream-function formulation which requires the solution of the scalar fourth-order equation

$$\mathrm{L}_{-1}^2 \psi = 0, \tag{3}$$

where L_{-1} is the axisymmetric Stokes operator. In a cylindrical coordinate system, it can be written as

$$\mathrm{L}_{-1} = \frac{\partial^2}{\partial r^2} - \frac{1}{r}\frac{\partial}{\partial r} + \frac{\partial^2}{\partial z^2}, \tag{4}$$

where (z, r) are the usual cylindrical coordinates.

Since the interfaces of the drop are assumed to be of uniform curvature, and the configuration of the drop exactly fits the toroidal coordinate system, we shall cast the Stokes equation in that coordinate system. This system has been highly useful in the treatment of fluid flow problems involving lens-shaped axisymmetric bodies (see Payne & Pell 1960; Majumdar, O'Neill & Brenner 1974). The toroidal coordinates (ξ, η) are related to the cylindrical coordinates (r, z) by the following transformation:

$$r = \frac{c \sinh \xi}{\cosh \xi - \cos \eta} \tag{5}$$

$$z = \frac{c \sin \eta}{\cosh \xi - \cos \eta} \qquad (0 < \xi < \infty; \quad -\pi < \eta < \pi). \tag{6}$$

The interfaces are identified by constant values of η, i.e. $\eta = \eta_{12}$, η_{13} and η_{23}, where the subscripts correspond to the respective interfaces as shown in figure 1. The velocity components are given by

$$[u_\xi, u_\eta] = \frac{(\cosh \xi - \cos \eta)^2}{c^2 \sinh \xi}\left(\frac{\partial \psi}{\partial \eta}, -\frac{\partial \psi}{\partial \xi}\right) \tag{7}$$

and the shear stress is written as

$$\tau_{\xi\eta} = \mu\left[(\cosh \xi - \cos \eta)\left(\frac{\partial u_\xi}{\partial \eta} + \frac{\partial u_\eta}{\partial \xi}\right) + u_\xi \sin \eta + u_\eta \sinh \xi\right]. \tag{8}$$

We now introduce the following non-dimensional variables:

$$u_\xi^* = \frac{u_\xi}{U_\infty}, \quad u_\eta^* = \frac{u_\eta}{U_\infty}, \quad \psi^* = \frac{\psi}{c^2 U_\infty}, \tag{9}$$

and then drop the asterisks. The solution for the Stokes equation (3) in a toroidal coordinate system (ξ, η) can be obtained by assuming a stream function of the following form:

$$\psi(\xi, \eta) = \frac{1}{(\cosh \xi - \cos \eta)^{\frac{3}{2}}} \Phi(\xi, \eta) \tag{10}$$

$$= \frac{1}{(\cosh \xi - \cos \eta)^{\frac{3}{2}}} \int_0^\infty \hat{\phi}(\eta, \lambda) \sinh^2 \xi \, P'_{-\frac{1}{2}+i\lambda}(\cosh \xi) \, \mathrm{d}\lambda, \tag{11}$$

where $\hat{\phi}(\eta, \lambda)$ is a combination of four linearly independent solutions,

$$\hat{\phi}(\eta,\lambda) = \cos\eta[A^*(\lambda)\cosh\lambda\eta + B^*(\lambda)\sinh\lambda\eta] + \sin\eta[C^*(\lambda)\cosh\lambda\eta + D^*(\lambda)\sinh\lambda\eta]. \quad (12)$$

In this solution, $P'_{-\frac{1}{2}+i\lambda}(\cosh\xi)$ is the derivative of the Legendre function, and the coefficients $A^*(\lambda), B^*(\lambda), C^*(\lambda), D^*(\lambda)$ are to be determined by the boundary conditions.

It is convenient to work with $\Phi(\xi, \eta)$ as the dependent variable instead of $\psi(\xi, \eta)$. Therefore, we express the velocities and the shear stress in terms of $\Phi(\xi, \eta)$. The velocities are

$$u_\xi = -\frac{3}{2}\frac{\sin\eta}{\sinh\xi(\cosh\xi-\cos\eta)^{\frac{1}{2}}}\Phi + \frac{(\cosh\xi-\cos\eta)^{\frac{1}{2}}}{\sinh\xi}\frac{\partial\Phi}{\partial\eta}, \quad (13)$$

$$u_\eta = \frac{3}{2}\frac{1}{(\cosh\xi-\cos\eta)^{\frac{1}{2}}}\Phi - \frac{(\cosh\xi-\cos\eta)^{\frac{1}{2}}}{\sinh\xi}\frac{\partial\Phi}{\partial\xi}. \quad (14)$$

The shear stress can then be expressed as

$$\tau_{\xi\eta} = \mu\left[\frac{(\cosh\xi-\cos\eta)^{\frac{3}{2}}}{\sinh\xi}\left(\frac{\partial^2\Phi}{\partial\eta^2} - \frac{\partial^2\Phi}{\partial\xi^2}\right) + (\cosh\xi-\cos\eta)^{\frac{3}{2}}\frac{\cosh\xi}{\sinh^2\xi}\frac{\partial\Phi}{\partial\xi} + \frac{1}{\sinh\xi(\cosh\xi-\cos\eta)^{\frac{1}{2}}}\{-\tfrac{3}{2}(\cosh\xi-\cos\eta)\cos\eta - \tfrac{3}{4}\sin^2\eta + \tfrac{3}{4}\sinh^2\xi\}\Phi\right]. \quad (15)$$

These expressions will be used later for satisfying the interface conditions.

Since the Stokes stream function obeys a linear partial differential equation, different flow fields can be solved separately and later combined to form the complete solution. Therefore, for convenience, the solutions are decomposed into two parts: a flow field resulting from the translation of the drop and a flow field resulting from the moving boundaries of the drop due to the growth. The stream functions in the two liquid phases can thus be expressed as

$$\psi_i(\xi,\eta) = \psi_i^{(t)}(\xi,\eta) + \psi_i^{(g)}(\xi,\eta) \quad (i = 1, 2) \quad (16)$$

where the superscripts t and g refer to translation and growth, respectively. The subscripts 1 and 2 correspond to the continuous and the dispersed liquid phases, respectively. Clearly, we may also write

$$\Phi_i(\xi,\eta) = \Phi_i^{(t)}(\xi,\eta) + \Phi_i^{(g)}(\xi,\eta) \quad (i = 1, 2). \quad (17)$$

3.1. *Translational flow field*

The solution for the continuous phase can be written as

$$\psi_1^{(t)}(\xi,\eta) = \frac{1}{(\cosh\xi-\cos\eta)^{\frac{3}{2}}}\int_0^\infty \hat{\phi}_1^{(t)}(\eta,\lambda)\sinh^2\xi\, P'_{-\frac{1}{2}+i\lambda}(\cosh\xi)\,d\lambda, \quad (18)$$

where

$$\phi_1^{(t)}(\eta,\lambda) = F(\eta,\lambda) + \cos\eta[A_t^*(\lambda)\cosh\lambda\eta + B_t^*(\lambda)\sinh\lambda\eta] + \sin\eta[C_t^*(\lambda)\cosh\lambda\eta + D_t^*(\lambda)\sinh\lambda\eta]. \quad (19)$$

In this expression, $F(\eta, \lambda)$ appears from the expansion

$$\frac{1}{2}\left[\frac{1}{(\cosh\xi-\cos\eta)^{\frac{1}{2}}} - \frac{1}{(\cosh\xi+\cos\eta)^{\frac{1}{2}}}\right] = \int_0^\infty F(\eta,\lambda)\,P'_{-\frac{1}{2}+i\lambda}(\cosh\xi)\,d\lambda, \quad (20)$$

where the first term on the left arises from the uniform stream. The detailed derivation is given in the Appendix.† As explained there, an expansion for just the uniform stream leads to difficulties and the additional term is necessary for the integral expansion. The expressions for $F(\eta,\lambda)$, $F'(\eta,\lambda)$ and $F''(\eta,\lambda)$ are found to be

$$\left.\begin{aligned} F(\eta,\lambda) &= \frac{-\cos\eta[\cosh\lambda(\pi-|\eta|)+\cosh\lambda\eta]}{\sqrt{2}(1+\lambda^2)\cosh\lambda\pi} \\ &\quad + \frac{\lambda\sin|\eta|[\sinh\lambda(\pi-|\eta|)+\sinh\lambda|\eta|]}{\sqrt{2}(1+\lambda^2)\cosh\lambda\pi}, \qquad (21) \\ F'(\eta,\lambda) &= \frac{\sin\eta[\cosh\lambda(\pi-|\eta|)+\cosh\lambda\eta]}{\sqrt{2}\cosh\lambda\pi}, \qquad (22) \\ F''(\eta,\lambda) &= \frac{\cos\eta[\cosh\lambda(\pi-|\eta|)+\cosh\lambda\eta]}{\sqrt{2}\cosh\lambda\pi} \\ &\quad + \frac{\lambda\sin|\eta|[-\sinh\lambda(\pi-|\eta|)+\sinh\lambda|\eta|]}{\sqrt{2}\cosh\lambda\pi}, \qquad (23) \end{aligned}\right\} \quad -\pi<\eta<\pi,$$

where the primes stand for $\partial/\partial\eta$.

The solution for motion of the dispersed-phase liquid can be written as

$$\psi_2^{(t)}(\xi,\eta) = \frac{1}{(\cosh\xi-\cos\eta)^{\frac{3}{2}}}\int_0^\infty \hat{\phi}_2^{(t)}(\eta,\lambda)\sinh^2\xi P'_{-\frac{1}{2}+i\lambda}(\cosh\xi)\,d\lambda, \qquad (24)$$

where

$$\hat{\phi}_2(\eta,\lambda) = \cos\eta[E_t^*(\lambda)\cosh\lambda\eta + F_t^*(\lambda)\sinh\lambda\eta] + \sin\eta[G_t^*(\lambda)\cosh\lambda\eta + H_t^*(\lambda)\sinh\lambda\eta]. \qquad (25)$$

The coefficients $A_t^*(\lambda), B_t^*(\lambda), C_t^*(\lambda), D_t^*(\lambda), E_t^*(\lambda), F_t^*(\lambda), G_t^*(\lambda), H_t^*(\lambda)$ are determined from the boundary conditions.

3.1.1. *Boundary conditions for translation*

(i) Constant stream-function value at boundaries $\eta = \eta_{13}, \eta_{12}, \eta_{23}$:

$$\hat{\phi}_1^{(t)}(\eta_{13},\lambda) = \hat{\phi}_1^{(t)}(\eta_{12},\lambda) = \hat{\phi}_2^{(t)}(\eta_{12},\lambda) = \hat{\phi}_2^{(t)}(\eta_{23},\lambda) = 0. \qquad (26)$$

(ii) Zero shear stress at boundaries $\eta = \eta_{13}, \eta_{23}$:

$$\hat{\phi}_1^{(t)\prime\prime}(\eta_{13},\lambda) = \hat{\phi}_2^{(t)\prime\prime}(\eta_{23},\lambda) = 0. \qquad (27)$$

(iii) Continuity of tangential velocity at boundary $\eta = \eta_{12}$:

$$\hat{\phi}_1^{(t)\prime}(\eta_{12},\lambda) = \hat{\phi}_2^{(t)\prime}(\eta_{12},\lambda). \qquad (28)$$

(iv) Continuity of shear stress at boundary $\eta = \eta_{12}$:

$$\mu_1\hat{\phi}_1^{(t)\prime\prime}(\eta_{12},\lambda) = \mu_2\hat{\phi}_2^{(t)\prime\prime}(\eta_{12},\lambda). \qquad (29)$$

Here again, the primes stand for $\partial/\partial\eta$. With these eight boundary and interface conditions, the eight unknown coefficients can then be determined. Instead of using

† The Appendix consisting of various integral expansions is available upon request from the Editor or from the authors.

the general solutions as given by (19) and (25), we choose the following form for functions $\hat{\phi}_1^{(t)}(\eta,\lambda)$ and $\hat{\phi}_2^{(t)}(\eta,\lambda)$:

$$\hat{\phi}_1^{(t)}(\eta,\lambda) = F(\eta,\lambda)$$
$$+A_t(\lambda)\left[\frac{\cos(\eta-\eta_{12})\sinh\lambda(\eta-\eta_{12})}{\cos(\eta_{13}-\eta_{12})\sinh\lambda(\eta_{13}-\eta_{12})}-\frac{\sin(\eta-\eta_{12})\cosh\lambda(\eta-\eta_{12})}{\sin(\eta_{13}-\eta_{12})\cosh\lambda(\eta_{13}-\eta_{12})}\right]$$
$$+B_t(\lambda)\left[\frac{\cos(\eta_{13}-\eta)\sinh\lambda(\eta_{13}-\eta)}{\cos(\eta_{13}-\eta_{12})\sinh\lambda(\eta_{13}-\eta_{12})}-\frac{\sin(\eta_{13}-\eta)\cosh\lambda(\eta_{13}-\eta)}{\sin(\eta_{13}-\eta_{12})\cosh\lambda(\eta_{13}-\eta_{12})}\right]$$
$$-F(\eta_{13},\lambda)\left[\cos(\eta-\eta_{13})\frac{\sinh\lambda(\eta-\eta_{12})}{\sinh\lambda(\eta_{13}-\eta_{12})}\right]-F(\eta_{12},\lambda)\left[\cos(\eta_{12}-\eta)\frac{\sinh\lambda(\eta_{13}-\eta)}{\sinh\lambda(\eta_{13}-\eta_{12})}\right], \tag{30}$$

which satisfies $\hat{\phi}_1^{(t)}(\eta_{13},\lambda)=\hat{\phi}_1^{(t)}(\eta_{12},\lambda)=0$; and

$$\hat{\phi}_2^{(t)}(\eta,\lambda) = C_t(\lambda)\left[\frac{\cos(\eta-\eta_{12})\sinh\lambda(\eta-\eta_{12})}{\cos(\eta_{23}-\eta_{12})\sinh\lambda(\eta_{23}-\eta_{12})}-\frac{\sin(\eta-\eta_{12})\cosh\lambda(\eta-\eta_{12})}{\sin(\eta_{23}-\eta_{12})\cosh\lambda(\eta_{23}-\eta_{12})}\right]$$
$$+D_t(\lambda)\left[\frac{\cos(\eta_{23}-\eta)\sinh\lambda(\eta_{23}-\eta)}{\cos(\eta_{23}-\eta_{12})\sinh\lambda(\eta_{23}-\eta_{12})}-\frac{\sin(\eta_{23}-\eta)\cosh\lambda(\eta_{23}-\eta)}{\sin(\eta_{23}-\eta_{12})\cosh\lambda(\eta_{23}-\eta_{12})}\right], \tag{31}$$

which satisfies $\hat{\phi}_2^{(t)}(\eta_{12},\lambda)=\hat{\phi}_2^{(t)}(\eta_{23},\lambda)=0$. The four coefficients $A_t(\lambda)$, $B_t(\lambda)$, $C_t(\lambda)$, $D_t(\lambda)$ are determined by satisfying the remaining four boundary conditions. After a great deal of algebra, we obtain:

$$A_t(\lambda) = \frac{F''(\eta_{13},\lambda)-F(\eta_{13},\lambda)(\lambda^2-1)-2\lambda(\sin\theta_1/\sinh\lambda\theta_1)F(\eta_{12},\lambda)}{2\lambda(\tan\theta_1\coth\lambda\theta_1+\cot\theta_1\tanh\lambda\theta_1)}, \tag{32}$$

$$B_t(\lambda) = \frac{c_1(\lambda)b_2(\lambda)-c_2(\lambda)b_1(\lambda)}{a_1(\lambda)b_2(\lambda)-a_2(\lambda)b_1(\lambda)}, \tag{33}$$

$$C_t(\lambda) = 0, \tag{34}$$

$$D_t(\lambda) = \frac{a_1(\lambda)c_2(\lambda)-a_2(\lambda)c_1(\lambda)}{a_1(\lambda)b_2(\lambda)-a_2(\lambda)b_1(\lambda)}, \tag{35}$$

where
$$\theta_1=\eta_{13}-\eta_{12},\quad \theta_2=\eta_{23}-\eta_{12},\quad \sigma_\mu=\mu_1/\mu_2, \tag{36}$$

$$a_1(\lambda) = \tan\theta_1-\lambda\coth\lambda\theta_1+\cot\theta_1+\lambda\tanh\lambda\theta_1, \tag{37}$$

$$b_1(\lambda) = -(\tan\theta_2-\lambda\coth\lambda\theta_2+\cot\theta_2+\lambda\tanh\lambda\theta_2), \tag{38}$$

$$c_1(\lambda) = \lambda F(\eta_{13},\lambda)\frac{\cos\theta_1}{\sinh\lambda\theta_1}-\lambda F(\eta_{12},\lambda)\coth\lambda\theta_1-F'(\eta_{12},\lambda)$$
$$-A_t(\lambda)\left(\frac{\lambda}{\cos\theta_1\sinh\lambda\theta_1}-\frac{1}{\sin\theta_1\cosh\lambda\theta_1}\right), \tag{39}$$

$$a_2(\lambda) = \sigma_\mu(\tan\theta_1\coth\lambda\theta_1+\cot\theta_1\tanh\lambda\theta_1), \tag{40}$$

$$b_2(\lambda) = -(\tan\theta_2\coth\lambda\theta_2+\cot\theta_2\tanh\lambda\theta_2), \tag{41}$$

$$c_2(\lambda) = \frac{\sigma_\mu}{2\lambda}F''(\eta_{12},\lambda)-\sigma_\mu\frac{\lambda^2-1}{2\lambda}F(\eta_{12},\lambda)-\sigma_\mu F(\eta_{13},\lambda)\frac{\sin\theta_1}{\sinh\lambda\theta_1}. \tag{42}$$

3.2. *Flow field resulting from the growth of the drop*

As stated earlier, the growth of the drop is separated into two parts: (i) growth resulting from the angular motion of the interfaces about the contact circle ($\dot{\eta}$); and (ii) growth resulting from the increasing radius of the contact circle ($\dot{c}$) as shown in figure 2. The two velocities $\dot{c}$ and $\dot{\eta}$ cannot vary independently but are related by the imposition of the total mass conservation of the liquid and the vapour. Bearing in mind that the liquid-to-vapour density ratio is approximately 10^3 under atmospheric conditions, we may let the liquid-side velocity of the liquid–vapour interface be equal to velocity of the interface itself. In addition, the conservation of mass leads to the condition that the volume of the unevaporated portion of the liquid phase of the drop must remain instantaneously constant while the drop shape is changing to a new configuration.

The volume of the liquid phase can be written as

$$V_1 = V(\eta_{12}) - V(\eta_{23}), \tag{43}$$

where

$$V(\eta) = \tfrac{1}{6}\pi c^3 \left[\frac{3\sin\eta}{1-\cos\eta} + \frac{\sin^3\eta}{(1-\cos\eta)^3}\right] \tag{44}$$

is the volume of a spherical segment. By imposing the volume of the liquid phase to be constant $\dot{V}_1 = 0$ and carrying out the algebra, we obtain

$$c\dot{\eta}\left[\frac{1}{(1-\cos\eta_{23})^2} - \frac{1}{(1-\cos\eta_{12})^2}\right] = \frac{\dot{c}\sin\eta_{23}(2-\cos\eta_{23})}{(1-\cos\eta_{23})^2} - \frac{\dot{c}\sin\eta_{12}(2-\cos\eta_{12})}{(1-\cos\eta_{12})^2}. \tag{45}$$

Using the following non-dimensional variables:

$$\dot{\eta}^* = \frac{c\dot{\eta}}{U_\infty}, \quad \dot{c}^* = \frac{\dot{c}}{U_\infty} \tag{46}$$

and dropping the asterisks, we obtain the relationship between $\dot{c}$ and $\dot{\eta}$ as follows:

$$\dot{\eta}\left[\frac{1}{(1-\cos\eta_{23})^2} - \frac{1}{(1-\cos\eta_{12})^2}\right] = \frac{\dot{c}\sin\eta_{23}(2-\cos\eta_{23})}{(1-\cos\eta_{23})^2} - \frac{\dot{c}\sin\eta_{12}(2-\cos\eta_{12})}{(1-\cos\eta_{12})^2}. \tag{47}$$

We now derive the stream-function values on the interfaces arising from these boundary velocities.

3.2.1. *Boundary velocities due to* $\dot{\eta}$

Holding c constant, we have

$$\left.\begin{aligned} \mathrm{d}s = \frac{c}{\cosh\xi - \cos\eta}\mathrm{d}\eta \Rightarrow \dot{s} = \frac{c}{\cosh\xi - \cos\eta}\dot{\eta}, \\ u_\eta = -\frac{(\cosh\xi - \cos\eta)^2}{c^2\sinh\xi}\frac{\partial\psi_{\dot{\eta}}^{(\mathrm{g})}}{\partial\xi} = \frac{c\dot{\eta}}{\cosh\xi - \cos\eta}. \end{aligned}\right\} \tag{48}$$

After non-dimensionalizing and dropping the asterisks, one gets

$$\frac{\partial\psi_{\dot{\eta}}^{(\mathrm{g})}}{\partial\xi} = -\frac{\dot{\eta}\sinh\xi}{(\cosh\xi - \cos\eta)^3}.$$

Integration with respect to ξ gives

$$\psi_{\dot{\eta}}^{(g)} = \frac{1}{2}\frac{\dot{\eta}}{(\cosh\xi - \cos\eta)^2} \quad \text{or} \quad \Phi_{\dot{\eta}}^{(g)} = \frac{1}{2}\frac{\dot{\eta}}{(\cosh\xi - \cos\eta)^{\frac{1}{2}}} \tag{49}$$

on the free surfaces.

3.2.2. *Boundary velocities due to* $\dot{c}$

Holding η constant this time,

$$\dot{r} = u_r = \frac{\dot{c}\sinh\xi}{\cosh\xi - \cos\eta}; \quad \dot{z} = u_z = \frac{\dot{c}\sin\eta}{\cosh\xi - \cos\eta}. \tag{50}$$

The transformation of the velocities u_r and u_z from cylindrical to toroidal coordinates u_ξ and u_η yields

$$u_\xi = -\frac{\dot{c}\sinh\xi\cos\eta}{\cosh\xi - \cos\eta}; \quad u_\eta = -\frac{\dot{c}\cosh\xi\sin\eta}{\cosh\xi - \cos\eta}. \tag{51}$$

We only take into account the normal velocity contribution but ignore the tangential velocity since the tangential component can be lumped into the solution for the translation of the drop. Thus,

$$u_\eta = -\frac{(\cosh\xi - \cos\eta)^2}{c^2\sinh\xi}\frac{\partial\psi_{\dot{c}}^{(g)}}{\partial\xi} = -\frac{\dot{c}\cosh\xi\sin\eta}{\cosh\xi - \cos\eta}. \tag{52}$$

After non-dimensionalizing and dropping the asterisks, one obtains

$$\frac{\partial\psi_{\dot{c}}^{(g)}}{\partial\xi} = \frac{\dot{c}\sin\eta\sinh\xi\cosh\xi}{(\cosh\xi - \cos\eta)^3}. \tag{53}$$

Integration with respect to ξ gives

$$\psi_{\dot{c}}^{(g)} = -\frac{1}{2}\frac{\dot{c}\sin\eta\cos\eta}{(\cosh\xi - \cos\eta)^2} - \frac{\dot{c}\sin\eta}{\cosh\xi - \cos\eta} \tag{54}$$

or

$$\Phi_{\dot{c}}^{(g)} = -\frac{1}{2}\frac{\dot{c}\sin\eta\cos\eta}{(\cosh\xi - \cos\eta)^{\frac{1}{2}}} - \dot{c}\sin\eta(\cosh\xi - \cos\eta)^{\frac{1}{2}} \tag{55}$$

on the free surfaces.

Combining the two boundary conditions resulting from $\dot{\eta}$ and $\dot{c}$ forms set of total boundary conditions for $\Phi^{(g)}$ at the interfaces,

$$\Phi_{BC}^{(g)} = \frac{1}{2}\frac{\dot{\eta} - \dot{c}\sin\eta\cos\eta}{(\cosh\xi - \cos\eta)^{\frac{1}{2}}} - \dot{c}\sin\eta(\cosh\xi - \cos\eta)^{\frac{1}{2}}, \tag{56}$$

where η is equal to η_{12}, η_{13} or η_{23}. By substituting the above expression for $\Phi_{BC}^{(g)}$ into the shear stress equation (15), we obtain

$$\tau_{\xi\eta}|_{BC} = \mu\frac{(\cosh\xi - \cos\eta)^{\frac{3}{2}}}{\sinh\xi}\left[\left.\frac{\partial^2\Phi^{(g)}}{\partial\eta^2}\right|_{BC.} - \tfrac{3}{8}\sin^2\eta\frac{\dot{\eta} - \dot{c}\sin\eta\cos\eta}{(\cosh\xi - \cos\eta)^{\frac{5}{2}}}\right.$$
$$\left. + \frac{3}{4}\frac{\dot{c}\sin\eta - \dot{\eta}\cos\eta}{(\cosh\xi - \cos\eta)^{\frac{3}{2}}} + \frac{3}{2}\frac{\dot{c}\sin\eta\cos\eta}{(\cosh\xi - \cos\eta)^{\frac{1}{2}}} - \frac{\dot{c}\sin\eta\sinh^2\xi}{(\cosh\xi - \cos\eta)^{\frac{3}{2}}}\right], \tag{57}$$

where again η can be chosen to represent any of the interfaces. The expressions for $\Phi_{BC}^{(g)}$ and $\tau_{\xi\eta}|_{BC}$ at the interfaces must be presented in the form of the general solution

of the Stokes equation so that the boundary conditions can be applied. In other words, we wish to expand (56) and (57) in the following form:

$$\Phi^{(g)}_{BC} = \int_0^\infty \mathscr{M}(\eta,\lambda)\sinh^2\xi P'_{-\frac{1}{2}+i\lambda}(\cosh\xi)\,d\lambda, \tag{58}$$

$$\tau_{\xi\eta}|_{BC} = \mu\frac{(\cosh\xi-\cos\eta)^{\frac{3}{2}}}{\sinh\xi}\left[\frac{\partial^2\Phi^{(g)}}{\partial\eta^2}\bigg|_{BC} - \int_0^\infty \mathscr{N}(\eta,\lambda)\sinh^2\xi P'_{-\frac{1}{2}+i\lambda}(\cosh\xi)\,d\lambda\right], \tag{59}$$

where the two functions $\mathscr{M}(\eta,\lambda)$ and $\mathscr{N}(\eta,\lambda)$ are to be determined. It should be noted that $\partial^2\Phi^{(g)}/\partial\eta^2$ is still an unknown function.

To expand the expression for $\Phi^{(g)}_{BC}$ as given in (56) we need to use the integral expansions of $(\cosh\xi-\cos\eta)^{\frac{1}{2}}$ and $(\cosh\xi-\cos\eta)^{-\frac{1}{2}}$. These are given by

$$(\cosh\xi-\cos\eta)^{\frac{1}{2}} = -\int_0^\infty \frac{1}{\lambda^2+\frac{1}{4}}\left[\lambda\tanh\lambda\pi(1-\cos\eta)^{\frac{1}{2}} + \frac{1}{\sqrt{2}}\frac{1\cosh\lambda(\pi-|\eta|)}{\cosh\lambda\pi}\right]\sinh^2\xi P'_{-\frac{1}{2}+i\lambda}(\cosh\xi)\,d\lambda \quad (-\pi<\eta<\pi) \tag{60}$$

and

$$\frac{1}{(\cosh\xi-\cos\eta)^{\frac{1}{2}}} = \int_0^\infty \frac{\lambda}{\lambda^2+\frac{1}{4}}\left[\frac{\sqrt{2}\sinh\lambda(\pi-|\eta|)}{\sin|\eta|\cosh\lambda\pi} - \frac{\tanh\lambda\pi}{(1-\cos\eta)^{\frac{1}{2}}}\right]\sinh^2\xi P'_{-\frac{1}{2}+i\lambda}(\cosh\xi)\,d\lambda \quad (-\pi<\gamma<\pi). \tag{61}$$

The detailed derivations are given in the Appendix which is available upon request (see earlier footnote in §3.1). By linearly combining the two expansions, one can obtain the expansion for the right-hand side of (56). As a result, we can identify $\mathscr{M}(\eta,\lambda)$ as

$$\mathscr{M}(\eta,\lambda) = \frac{1}{2}\frac{\lambda}{(\lambda^2+\frac{1}{4})}(\dot\eta-\dot c\sin\eta\cos\eta)\left[\frac{\sqrt{2}\sinh\lambda(\pi-|\eta|)}{\sin|\eta|\cosh\lambda\pi} - \frac{\tanh\lambda\pi}{(1-\cos\eta)^{\frac{1}{2}}}\right] + \frac{\dot c\sin\eta}{\lambda^2+\frac{1}{4}}\left[\frac{\cosh\lambda(\pi-|\eta|)}{\sqrt{2}\cosh\lambda\pi} + \lambda\tanh\lambda\pi\,(1-\cos\eta)^{\frac{1}{2}}\right]. \tag{62}$$

Similarly, for $\tau_{\xi\eta}|_{BC}$, we use the integral expansions for $(\cosh\xi-\cos\eta)^{-\frac{1}{2}}$, $(\cosh\xi-\cos\eta)^{-\frac{3}{2}}$ and $(\cosh\xi-\cos\eta)^{-\frac{5}{2}}$. The expansions for the last two expressions have also been derived in the Appendix. These are given by

$$\frac{1}{(\cosh\xi-\cos\eta)^{\frac{3}{2}}} = \int_0^\infty \frac{\lambda}{\lambda^2+\frac{1}{4}}\left[\frac{2\sqrt{2}}{\sin^3|\eta|\cosh\lambda\pi}\times\{\lambda\sin|\eta|\cosh\lambda(\pi-|\eta|)+\cos\eta\sinh\lambda(\pi-|\eta|)\} - \frac{\tanh\lambda\pi}{(1-\cos\eta)^{\frac{3}{2}}}\right]\times\sinh^2\xi P'_{-\frac{1}{2}+i\lambda}(\cosh\xi)\,d\lambda \quad (-\pi<\eta<\pi) \tag{63}$$

and

$$\frac{1}{(\cosh\xi-\cos\eta)^{\frac{5}{2}}}=\int_0^\infty \frac{\lambda}{\lambda^2+\frac{1}{4}}\left[\frac{4\sqrt{2}}{3\sin^5|\eta|\cosh\lambda\pi}\{3\cos\eta\sinh\lambda(\pi-|\eta|)\right.$$

$$\left.+(1+\lambda^2)\sin^2|\eta|\sinh\lambda(\pi-|\eta|)+3\lambda\sin|\eta|\cosh\lambda(\pi-|\eta|)\}-\frac{\tanh\lambda\pi}{(1-\cos\eta)^{\frac{5}{2}}}\right]$$

$$\times\sinh^2\xi P'_{-\frac{1}{2}+i\lambda}(\cosh\xi)\,d\lambda \quad (-\pi<\gamma<\pi). \tag{64}$$

Consequently, the expression for $\mathcal{N}(\eta,\lambda)$ can be written as

$$\mathcal{N}(\eta,\lambda)=\frac{3\lambda}{4(\lambda^2+\frac{1}{4})}(\dot\eta\cos\eta-\dot c\sin\eta)$$

$$\times\left[\frac{2\sqrt{2}}{\sin^3|\eta|\cosh\lambda\pi}\{\lambda\sin|\eta|\cosh\lambda(\pi-|\eta|)+\cos\eta\sinh\lambda(\pi-|\eta|)\}-\frac{\tanh\lambda\pi}{(1-\cos\eta)^{\frac{3}{2}}}\right]$$

$$+\frac{\lambda}{\lambda^2+\frac{1}{4}}(\dot\eta-\dot c\sin\eta\cos\eta)$$

$$\times\left[\frac{[3\cos\eta+(1+\lambda^2)\sin^2|\eta|]\sinh\lambda(\pi-|\eta|)+3\lambda\sin|\eta|\cosh\lambda(\pi-|\eta|)}{\sqrt{2}\sin^3|\eta|\cosh\lambda\pi}\right.$$

$$\left.-\frac{3\sin^2\eta\tanh\lambda\pi}{8(1-\cos\eta)^{\frac{5}{2}}}\right]-\frac{3\lambda}{2(\lambda^2+\frac{1}{4})}\dot c\sin\eta\cos\eta\left[\frac{\sqrt{2}\sinh\lambda(\pi-|\eta|)}{\sin|\eta|\cosh\lambda\pi}-\frac{\tanh\lambda\pi}{(1-\cos\eta)^{\frac{1}{2}}}\right]$$

$$-2\sqrt{2}\frac{\dot c\sin\eta\cosh\lambda(\pi-|\eta|)}{\cosh\lambda\pi}. \tag{65}$$

Now, referring to the continuous phase and the liquid dispersed phase by subscripts 1 and 2, respectively, we write the set of functions $\Phi_i^{(g)}(\xi,\eta)$ (see (17)) as

$$\Phi_i^{(g)}(\xi,\eta)=\int_0^\infty \hat\phi_i^{(g)}(\eta,\lambda)\sinh^2\xi P'_{-\frac{1}{2}+i\lambda}(\cosh\xi)\,d\lambda, \tag{66}$$

where

$$\hat\phi_1^{(g)}(\eta,\lambda)=\cos\eta[A_g^*(\lambda)\cosh\lambda\eta+B_g^*(\lambda)\sinh\lambda\eta]+\sin\eta[C_g^*(\lambda)\cosh\lambda\eta+D_g^*(\lambda)\sinh\lambda\eta] \tag{67}$$

and

$$\hat\phi_2^{(g)}(\eta,\lambda)=\cos\eta[E_g^*(\lambda)\cosh\lambda\eta+F_g^*(\lambda)\sinh\lambda\eta]+\sin\eta[G_g^*(\lambda)\cosh\lambda\eta+H_g^*(\lambda)\sinh\lambda\eta]. \tag{68}$$

Here, the coefficients, $A_g^*(\lambda)$, $B_g^*(\lambda)$, $C_g^*(\lambda)$, $D_g^*(\lambda)$, $E_g^*(\lambda)$, $F_g^*(\lambda)$, $G_g^*(\lambda)$ and $H_g^*(\lambda)$ are to be determined from the following boundary conditions:

(i) At the boundaries $\eta=\eta_{13},\eta_{12},\eta_{23}$, we have

$$\hat\phi_1^{(g)}(\eta_{13},\lambda)=\mathcal{M}(\eta_{13},\lambda),\quad \hat\phi_1^{(g)}(\eta_{12},\lambda)=\mathcal{M}(\eta_{12},\lambda), \tag{69}$$

$$\hat\phi_2^{(g)}(\eta_{12},\lambda)=\mathcal{M}(\eta_{12},\lambda),\quad \hat\phi_2^{(g)}(\eta_{23},\lambda)=\mathcal{M}(\eta_{23},\lambda), \tag{70}$$

where $\mathcal{M}(\eta,\lambda)$ is given by (62).

(ii) The conditions for zero shear stress at boundaries $\eta=\eta_{13},\eta_{23}$ require

$$\hat\phi_1^{(g)\prime\prime}(\eta_{13},\lambda)=\mathcal{N}(\eta_{13},\lambda),\quad \hat\phi_2^{(g)\prime\prime}(\eta_{23},\lambda)=\mathcal{N}(\eta_{23},\lambda), \tag{71}$$

where $\mathcal{N}(\eta,\lambda)$ is given by (65), and the double prime stands for $\partial^2/\partial\eta^2$.

(iii) The continuity of tangential velocity at boundary $\eta = \eta_{12}$ requires

$$\hat{\phi}_1^{(g)\prime}(\eta_{12}, \lambda) = \hat{\phi}_2^{(g)\prime}(\eta_{12}, \lambda), \tag{72}$$

where the single prime stands for $\partial/\partial\eta$.

(iv) The continuity of shear stress at boundary $\eta = \eta_{12}$ leads to

$$\mu_1[\hat{\phi}_1^{(g)\prime\prime}(\eta_{12}, \lambda) - \mathscr{N}(\eta_{12}, \lambda)] = \mu_2[\hat{\phi}_2^{(g)\prime\prime}(\eta_{12}, \lambda) - \mathscr{N}(\eta_{12}, \lambda)]. \tag{73}$$

We now choose the following forms for functions $\hat{\phi}_1^{(g)}(\eta, \lambda)$ and $\hat{\phi}_2^{(g)}(\eta, \lambda)$:

$$\begin{aligned}
&\hat{\phi}_1^{(g)}(\eta, \lambda) \\
&= A_g(\lambda)\left[\frac{\cos(\eta-\eta_{12})\sinh\lambda(\eta-\eta_{12})}{\cos(\eta_{13}-\eta_{12})\sinh\lambda(\eta_{13}-\eta_{12})} - \frac{\sin(\eta-\eta_{12})\cosh\lambda(\eta-\eta_{12})}{\sin(\eta_{13}-\eta_{12})\cosh\lambda(\eta_{13}-\eta_{12})}\right] \\
&\quad + B_g(\lambda)\left[\frac{\cos(\eta_{13}-\eta)\sinh\lambda(\eta_{13}-\eta)}{\cos(\eta_{13}-\eta_{12})\sinh\lambda(\eta_{13}-\eta_{12})} - \frac{\sin(\eta_{13}-\eta)\cosh\lambda(\eta_{13}-\eta)}{\sin(\eta_{13}-\eta_{12})\cosh\lambda(\eta_{13}-\eta_{12})}\right] \\
&\quad + \mathscr{M}(\eta_{13}, \lambda)\left[\cos(\eta-\eta_{13})\frac{\sinh\lambda(\eta-\eta_{12})}{\sinh\lambda(\eta_{13}-\eta_{12})}\right] + \mathscr{M}(\eta_{12}, \lambda)\left[\cos(\eta_{12}-\eta)\frac{\sinh\lambda(\eta_{13}-\eta)}{\sinh\lambda(\eta_{13}-\eta_{12})}\right]
\end{aligned} \tag{74}$$

and

$$\begin{aligned}
&\hat{\phi}_2(\eta, \lambda) \\
&= C_g(\lambda)\left[\frac{\cos(\eta-\eta_{12})\sinh\lambda(\eta-\eta_{12})}{\cos(\eta_{23}-\eta_{12})\sinh\lambda(\eta_{23}-\eta_{12})} - \frac{\sin(\eta-\eta_{12})\cosh\lambda(\eta-\eta_{12})}{\sin(\eta_{23}-\eta_{12})\cosh\lambda(\eta_{23}-\eta_{12})}\right] \\
&\quad + D_g(\lambda)\left[\frac{\cos(\eta_{23}-\eta)\sinh\lambda(\eta_{23}-\eta)}{\cos(\eta_{23}-\eta_{12})\sinh\lambda(\eta_{23}-\eta_{12})} - \frac{\sin(\eta_{23}-\eta)\cosh\lambda(\eta_{23}-\eta)}{\sin(\eta_{23}-\eta_{12})\cosh\lambda(\eta_{23}-\eta_{12})}\right] \\
&\quad + \mathscr{M}(\eta_{23}, \lambda)\left[\cos(\eta-\eta_{23})\frac{\sinh\lambda(\eta-\eta_{12})}{\sinh\lambda(\eta_{23}-\eta_{12})}\right] + \mathscr{M}(\eta_{12}, \lambda)\left[\cos(\eta_{12}-\eta)\frac{\sinh\lambda(\eta_{23}-\eta)}{\sinh\lambda(\eta_{23}-\eta_{12})}\right].
\end{aligned} \tag{75}$$

These forms are selected so that the boundary conditions given by (69) and (70) are satisfied. The four coefficients $A_g(\lambda)$, $B_g(\lambda)$, $C_g(\lambda)$, $D_g(\lambda)$ are determined from the remaining four boundary conditions given by (71)–(73). After some rather lengthy algebra, we obtain

$$A_g(\lambda) = \frac{\mathscr{M}(\eta_{13}, \lambda)(\lambda^2-1) + 2\lambda(\sin\theta_1/\sinh\lambda\theta_1)\mathscr{M}(\eta_{12}, \lambda) - \mathscr{N}(\eta_{13}, \lambda)}{2\lambda(\tan\theta_1\coth\lambda\theta_1 + \cot\theta_1\tanh\lambda\theta_1)}, \tag{76}$$

$$C_g(\lambda) = \frac{\mathscr{M}(\eta_{23}, \lambda)(\lambda^2-1) + 2\lambda(\sin\theta_2/\sinh\lambda\theta_2)\mathscr{M}(\eta_{12}, \lambda) - \mathscr{N}(\eta_{23}, \lambda)}{2\lambda(\tan\theta_2\coth\lambda\theta_2 + \cot\theta_2\tanh\lambda\theta_2)}, \tag{77}$$

$$B_g(\lambda) = \frac{c_1^*(\lambda)\,b_2(\lambda) - c_2^*(\lambda)\,b_1(\lambda)}{a_1(\lambda)\,b_2(\lambda) - a_2(\lambda)\,b_1(\lambda)}, \tag{78}$$

$$D_g(\lambda) = \frac{a_1(\lambda)\,c_2^*(\lambda) - a_2(\lambda)\,c_1^*(\lambda)}{a_1(\lambda)\,b_2(\lambda) - a_2(\lambda)\,b_1(\lambda)}, \tag{79}$$

where

$$\theta_1 = \eta_{13} - \eta_{12}, \quad \theta_2 = \eta_{23} - \eta_{12}, \quad \sigma_\mu = \frac{\mu_1}{\mu_2}, \tag{80}$$

$$c_1^*(\lambda) = C_g(\lambda)\left(\frac{\lambda}{\cos\theta_2 \sinh\lambda\theta_2} - \frac{1}{\sin\theta_2 \cosh\lambda\theta_2}\right) - A_g(\lambda)\left(\frac{\lambda}{\cos\theta_1 \sinh\lambda\theta_1} - \frac{1}{\sin\theta_1 \cosh\lambda\theta_1}\right)$$
$$+\lambda\mathscr{M}(\eta_{23},\lambda)\frac{\cos\theta_2}{\sinh\lambda\theta_2} - \lambda\mathscr{M}(\eta_{12},\lambda)\coth\lambda\theta_2 - \lambda\mathscr{M}(\eta_{13},\lambda)\frac{\cos\theta_1}{\sinh\lambda\theta_1}$$
$$+\lambda\mathscr{M}(\eta_{12},\lambda)\coth\lambda\theta_1, \tag{81}$$

$$c_2^*(\lambda) = \sigma_\mu \mathscr{M}(\eta_{12},\lambda)\frac{\sin\theta_1}{\sinh\lambda\theta_1} - \mathscr{M}(\eta_{23},\lambda)\frac{\sin\theta_2}{\sinh\lambda\theta_2}$$
$$+(\sigma_\mu - 1)\frac{\lambda^2-1}{2\lambda}\mathscr{M}(\eta_{12},\lambda) - (\sigma_\mu - 1)\frac{1}{2\lambda}\mathscr{N}(\eta_{12},\lambda), \tag{82}$$

and $a_1(\lambda)$, $a_2(\lambda)$, $b_1(\lambda)$ and $b_2(\lambda)$ are given by (37), (38), (40) and (41).

3.3. *Combined translational and growth flow field*

At this point, the combined flow field is simply a sum of the translational and the growth flow fields as expressed in (16). This yields the following expressions for the stream functions.

In the continuous phase we have

$$\psi_1(\xi,\eta) = \frac{\sinh^2\xi}{(\cosh\xi - \cos\eta)^{\frac{3}{2}}}\left\{\frac{1}{2}\left[\frac{1}{(\cosh\xi - \cos\eta)^{\frac{1}{2}}} - \frac{1}{(\cosh\xi + \cos\eta)^{\frac{1}{2}}}\right]\right.$$
$$\left. + \int_0^\infty \bar{\phi}_1(\eta,\lambda) P'_{-\frac{1}{2}+i\lambda}(\cosh\xi)\,d\lambda\right\}, \tag{83}$$

where

$$\bar{\phi}_1(\eta,\lambda) = [A_t(\lambda) + A_g(\lambda)]$$
$$\times\left[\frac{\cos(\eta-\eta_{12})\sinh\lambda(\eta-\eta_{12})}{\cos(\eta_{13}-\eta_{12})\sinh\lambda(\eta_{13}-\eta_{12})} - \frac{\sin(\eta-\eta_{12})\cosh\lambda(\eta-\eta_{12})}{\sin(\eta_{13}-\eta_{12})\cosh\lambda(\eta_{13}-\eta_{12})}\right]$$
$$+[B_t(\lambda) + B_g(\lambda)]\left[\frac{\cos(\eta_{13}-\eta)\sinh\lambda(\eta_{13}-\eta)}{\cos(\eta_{13}-\eta_{12})\sinh\lambda(\eta_{13}-\eta_{12})} - \frac{\sin(\eta_{13}-\eta)\cosh\lambda(\eta_{13}-\eta)}{\sin(\eta_{13}-\eta_{12})\cosh\lambda(\eta_{13}-\eta_{12})}\right]$$
$$+[\mathscr{M}(\eta_{13},\lambda) - F(\eta_{13},\lambda)]\left[\cos(\eta-\eta_{13})\frac{\sinh\lambda(\eta-\eta_{12})}{\sinh\lambda(\eta_{13}-\eta_{12})}\right]$$
$$+[\mathscr{M}(\eta_{12},\lambda) - F(\eta_{12},\lambda)]\left[\cos(\eta_{12}-\eta)\frac{\sinh\lambda(\eta_{13}-\eta)}{\sinh\lambda(\eta_{13}-\eta_{12})}\right]. \tag{84}$$

The coefficients $A_t(\lambda)$, $A_g(\lambda)$, $B_t(\lambda)$, $B_g(\lambda)$, $\mathscr{M}(\eta,\lambda)$ and $F(\eta,\lambda)$ are given in (21), (32), (33), (62), (76), (78).

Similarly, we obtain the stream function for the liquid region of the dispersed phase to be

$$\psi_2(\xi,\eta) = \frac{\sinh^2\xi}{(\cosh\xi - \cos\eta)^{\frac{3}{2}}}\int_0^\infty \bar{\phi}_2(\eta,\lambda) P'_{-\frac{1}{2}+i\lambda}(\cosh\xi)\,d\lambda, \tag{85}$$

where

$$\begin{aligned}\bar{\phi}_2(\eta,\lambda) &= C_g(\lambda)\left[\frac{\cos(\eta-\eta_{12})\sinh\lambda(\eta-\eta_{12})}{\cos(\eta_{23}-\eta_{12})\sinh\lambda(\eta_{23}-\eta_{12})}-\frac{\sin(\eta-\eta_{12})\cosh\lambda(\eta-\eta_{12})}{\sin(\eta_{23}-\eta_{12})\cosh\lambda(\eta_{23}-\eta_{12})}\right]\\ &+[D_g(\lambda)+D_i(\lambda)]\left[\frac{\cos(\eta_{23}-\eta)\sinh\lambda(\eta_{23}-\eta)}{\cos(\eta_{23}-\eta_{12})\sinh\lambda(\eta_{23}-\eta_{12})}-\frac{\sin(\eta_{23}-\eta)\cosh\lambda(\eta_{23}-\eta)}{\sin(\eta_{23}-\eta_{12})\cosh\lambda(\eta_{23}-\eta_{12})}\right]\\ &+\mathscr{M}(\eta_{23},\lambda)\left[\cos(\eta-\eta_{23})\frac{\sinh\lambda(\eta-\eta_{12})}{\sinh\lambda(\eta_{23}-\eta_{12})}\right]+\mathscr{M}(\eta_{12},\lambda)\left[\cos(\eta_{12}-\eta)\frac{\sinh\lambda(\eta_{23}-\eta)}{\sinh\lambda(\eta_{23}-\eta_{12})}\right].\end{aligned} \tag{86}$$

4. Results and discussion

The information on the flow velocities and drag force is useful for modelling the systems involving such compound drops. The results from the present analysis are applied to the heat transfer problem of the evaporating 3-singlet compound drop which is treated in Part 2. The discussion here is restricted to the basic aspects pertaining to the drag force and the flow field.

4.1. *The drag force*

Following Payne & Pell (1960) the expression for the drag force can be written as

$$\frac{P}{8\pi\mu cU_\infty}=\tfrac{1}{2}+\frac{1}{\sqrt{2}}\int_0^\infty \bar{\phi}_1(0,\lambda)(\lambda^2+\tfrac{1}{4})\,\mathrm{d}\lambda, \tag{87}$$

where the function $\bar{\phi}(0,\lambda)$ can be obtained from (84). Although the flow geometry consists of sharp corners at the moving contact line, Dussan-type non-integrable stress singularities (see Dussan V. 1973) are not present. This is because of the absence of any solid boundaries. The drag force is therefore finite.

As one would expect, the drag force on the compound drop depends on many parameters besides the viscosity of the continuous phase, the drop size and the free-stream velocity. Among the important parameters are the viscosity ratio $\sigma_\mu=\mu_1/\mu_2$ between the dispersed phase and the continuous phase; the drop geometry, i.e. the liquid to vapour volume ratio together with contact angles θ_1, θ_2, θ_3, which depend on the fluid systems being used; and the ratio of the growth to translational velocities, $\dot{c}/U_\infty$. Since this consists of five independent parameters, instead of producing elaborate tables with various values of each parameter, we restrict our discussion to a few special cases. A sample calculation of the drag force in the case without growth is shown in figure 3. We choose glycerol as the continuous phase and pentane as the dispersed phase with a set of contact angles $\theta_1=171°$, $\theta_2=32°$, $\theta_3=157°$ (refer to figure 1). The drag force is non-dimensionalized using a constant reference radius r_{ref} instead of the contact circle radius c, which varies with the drop configuration. Here we define r_{ref} as the radius of a sphere having the same volume as the compound drop, i.e.

$$\tfrac{4}{3}\pi r_{\mathrm{ref}}^3=V_l+V_v. \tag{88}$$

The drag force $P/(8\pi\mu_1 r_{\mathrm{ref}}U_\infty)$ is plotted against the liquid-to-vapour volume ratio V_l/V_v with the viscosity ratio $\sigma_\mu=\mu_1/\mu_2$ as a parameter. The total volume of the drop is kept constant while the liquid-to-vapour volume ratios are varied. Limiting cases

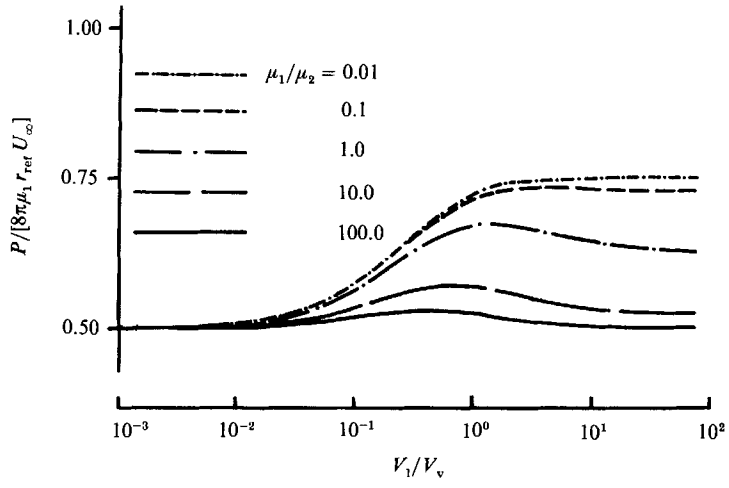

FIGURE 3. Drag force without growth.

of large or small volume ratios lead to liquid or vapour spheres, respectively. The plots show that in the limiting case of a drop consisting of mostly vapour, the drag force approaches the value for the bubble drag ($P = 4\pi\mu_1 r_{ref} U_\infty$). For a compound drop that is mostly liquid, we obtain the liquid sphere drag as given by the Rybczynski–Hadamard formula. For moderate liquid-to-vapour ratios, the plots exhibit humps showing a higher drag than that for a liquid sphere of volume ($V_l + V_v$) and viscosity μ_2. This appears to be a geometrical effect giving rise to greater resistance mostly due to the reduced available circulation space in the liquid portion of the dispersed phase. The deviation from sphericity in this particular configuration does not appear likely to cause this increase in drag, especially since the shape is elongated in the direction along the path of motion.

In figure 4, the drag force is plotted against volume ratio including both translation and growth. Here the growth rate $\dot{c}/U_\infty$ is chosen to be equal to 0.01 as an example. We see that the right-hand side of the curves changes very little as compared to the no-growth case in figure 3 while the left-hand sides of the curves move upward. This is actually an effect arising from the choice of the contact circle as a reference frame. With the velocities being relative to the centre of the contact circle, the non-uniform normal velocities at the interfaces from the growth of the drop result in a net translatory movement of the drop relative to the contact circle. This generates additional drag besides the drag resulting from the applied translational velocity U_∞. To obtain reasonable results we move the reference frame to the centroid of the compound drop. It is not difficult to obtain the centroid velocity, $\dot{d}$, once we have $\dot{c}$ and $\dot{\eta}$. The centroid velocity is plotted in figure 5. This velocity is in the opposite direction to that of the uniform stream, U_∞, and increases rapidly as the drop approaches vapour phase. By scaling the drag force with the velocity relative to the centroid of the drop, i.e. the velocity $(U_\infty - \dot{d})$ instead of U_∞, we obtained a familiar trend for the drag force, as shown in figure 6. Here we see that, with growth taking place, the middle hump for the moderate liquid-to-vapour ratio is more pronounced than for the case with no growth.

Nearly all of the experimental data on the drag involve heat transfer effects and therefore comparisons with the data have been made in Part 2.

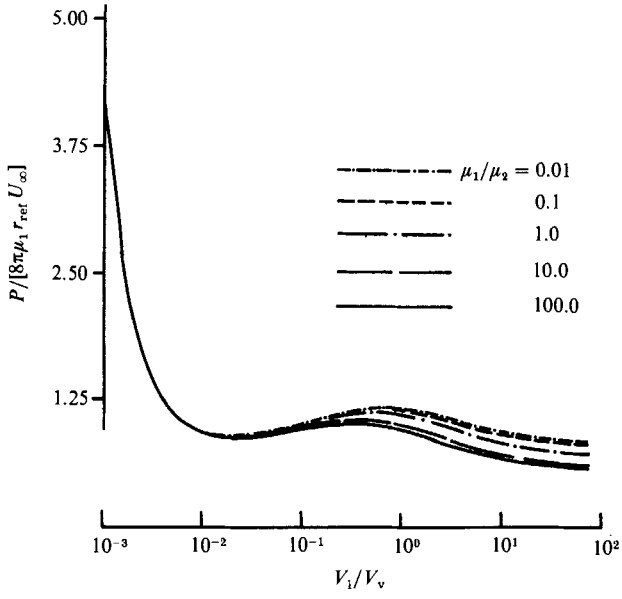

FIGURE 4. Drag force on a compound drop with growth ($\dot{c}/U_\infty = 0.01$).

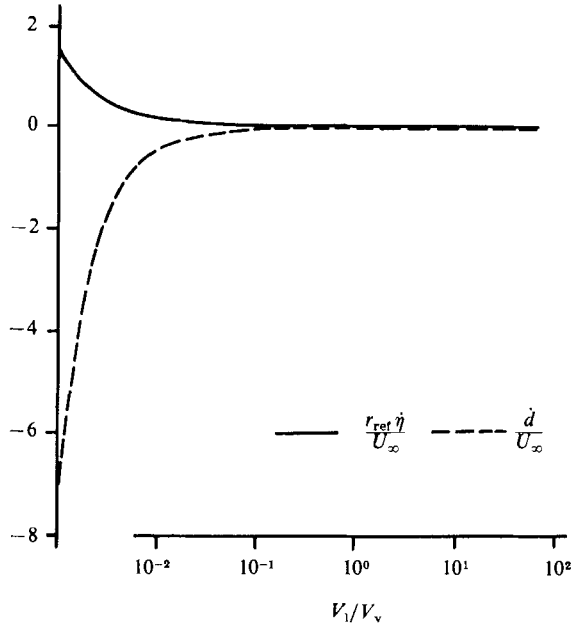

FIGURE 5. Centroid velocity as a function of volume ratio.

4.2. *The flow field*

In order to obtain the flow streamlines, one would require the numerical calculation of the integrals in (83) and (85). These calculations have been carried out by Oğuz's (1987) method which involved the use of hypergeometric function representation for $P_{-\frac{1}{2}+i\lambda}(\cosh\xi)$. The flow streamlines are presented separately for growth and

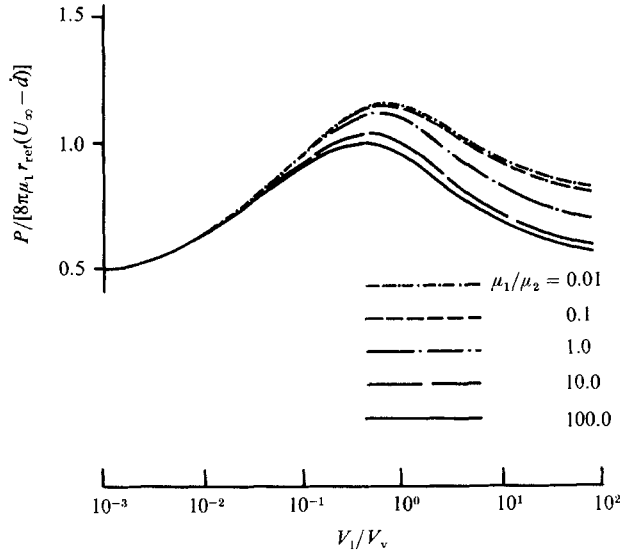

FIGURE 6. Drag force on a compound drop with growth ($\dot{c}/U_\infty = 0.01$) – centroid reference frame.

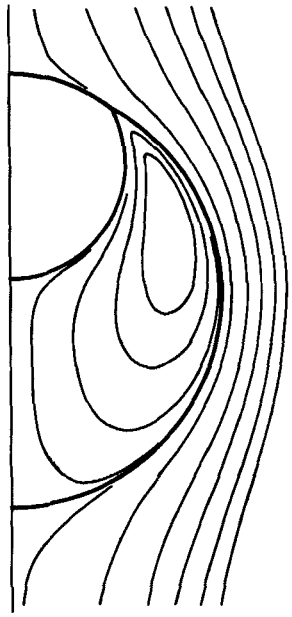

FIGURE 7. Streamlines for pure translation with large liquid volume.

translation along with the combined flow field. Figures 7–9 show the flow patterns when the dispersed phase is almost completely liquid. In figure 7 we see the translational flow field, which is more or less as expected. The effect of growth is seen in figure 8, where we observe the contribution of the angular velocity $\dot{\eta}$ by the outgoing streamlines at the interfaces. These streamlines are not normal to the interfaces because of the effect arising from $\dot{c}$ which causes a small amount of recirculation in the liquid part of the dispersed phase. The combined effect of translation and growth

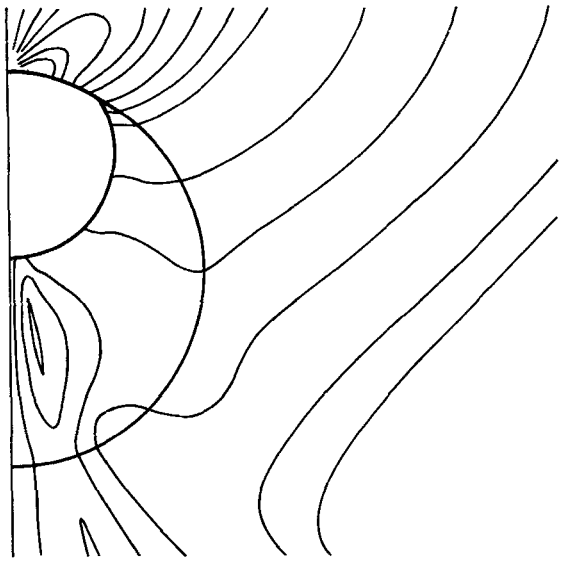

FIGURE 8. Streamlines for pure growth with large liquid volume.

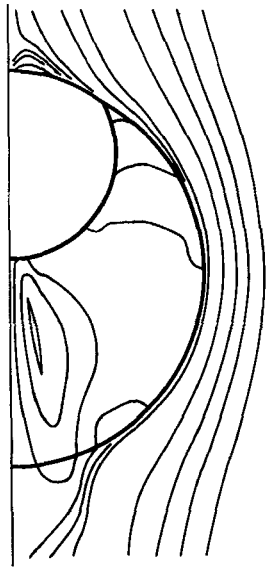

FIGURE 9. Streamlines for combined translation and growth with large liquid volume ($\dot{c}/U_\infty = 0.58$; $c\dot{\eta}/U_\infty = -0.28$).

is given in figure 9; the motion in the continuous phase shows minor influence from growth except for a small portion near the front and the rear stagnation points. However, the motion in the dispersed phase is still dominated by the growth.

When the liquid part of the dispersed phase is considerably smaller than the vapour, the buoyant force is likely to be large and therefore the translational velocities would be comparable with the growth velocities. The translational flow field is similar to the one shown in figure 7. The flow arising from growth, however, is somewhat different from the previous case. The flow streamlines are presented in figure 10. The combined effect growth and translation is given in figure 11. Because

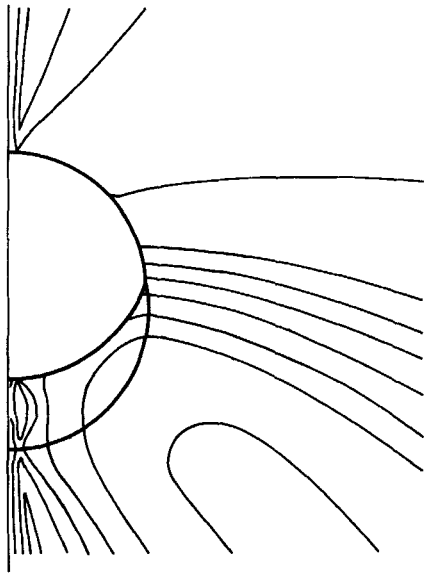

FIGURE 10. Streamlines for pure growth with small liquid volume.

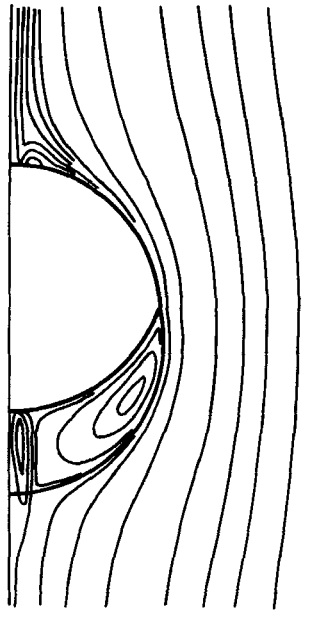

FIGURE 11. Combined translation and growth streamlines with small liquid volume ($\dot{c}/U_\infty = 0.094$; $c\dot{\eta}/U_\infty = -0.14$).

of greater translational velocity, the growth effect has a weaker role. The dominance of translation is seen in both the dispersed and the continuous phases. The effect of growth appears as a secondary vortex near the real stagnation point.

The authors are very grateful to the National Science Foundation for the support of this work under Grant No. CBT 83-51432. Thanks are also due to DAMTP (Cambridge University) for the availability of their research facilities to the second author (S.S.S.) who was on sabbatical leave there (5 July 1988–18 July 1989).

REFERENCES

AVEDISIAN, C. T. & ANDRES, R. P. 1978 Bubble nucleation in superheated liquid–liquid emulsions. *J. Colloid Interface Sci.* **64**, 438–453.

CHAMBERS, R. & KOPAC, M. J. 1937 The coalescence of living cells with oil drops. I. Arbacia eggs immersed in sea water. *J. Cell. Comp. Physiol.* **9**, 331–343.

DUSSAN, V., E. B. 1979 On the spreading of liquids on solid surfaces. *Ann. Rev. Fluid Mech.* **11**, 371–400.

HAYAKAWA, T. & SHIGETA, M. 1974 Terminal velocity of a two-phase droplet. *J. Chem. Engng Japan* **7**, 140–142.

JOHNSON, R. E. & SADHAL, S. S. 1963 Stokes flow past bubbles and drops partially coated with thin films. Part 2. Thin films with internal circulation – a perturbation solution. *J. Fluid Mech.* **132**, 295–318.

JOHNSON, R. E. & SADHAL, S. S. 1985 Fluid mechanics of compound multiphase drops and bubbles. *Ann. Rev. Fluid Mech.* **17**, 289–320.

KOPAC, M. J. & CHAMBERS, R. 1937 The coalescence of living cells with oil drops. II. Arbacia eggs immersed in acid or alkaline calcium solutions. *J. Cell Comp. Physiol.* **9**, 345–361.

LI, N. N. & ASHER, W. J. 1973 Blood oxygenation by liquid membrane permeation. In *Chemical Engineering in Medicine*. Advances in Chemistry Series, vol. 118, pp. 1–14.

MAJUMDAR, S. R., O'NEILL, M. E. & BRENNER, H. 1974 A note on the slow rotation of a convave spherical lens or bowl in two immescible semi-infinite viscous fluids. *Mathematika* **21**, 147–154.

MERCIER, J. L., DA CUNHA, F. M., TEIXEIRA, J. C. & SCHOFIELD, M. P. 1974 Influence of enveloping water layer on the rise of air bubbles in Newtonian fluids. *Trans. ASME* E: *J. Appl. Mech.* **96**, 29–34.

MORI, Y. H. 1978 Configuration of gas–liquid two-phase bubble in immiscible liquid media. *Intl J. Multiphase Flow* **4**, 383–396.

OĞUZ, H. N. 1987 Fluid dynamics of compound multiphase drops and bubbles. Ph.D. thesis, University of Southern California, Chap. 3.

OĞUZ, H. N. & SADHAL, S. S. 1987 Growth and collapse of translating compound multiphase drops: analysis of fluid mechanics and heat transfer. *J. Fluid Mech.* **179**, 105–136.

PAYNE, L. E. & PELL, W. W. 1960 The Stokes flow problem for a class of axially symmetric bodies. *J. Fluid Mech.* **7**, 529–549.

RUSHTON, E. & DAVIES, G. A. 1983 Settling of encapsulated droplets at low Reynolds numbers. *Intl J. Multiphase Flow* **9**, 337–342.

SADHAL, S. S. & OĞUZ, H. N. 1985 Stokes flow past compound multiphase drops: the case of completely engulfed drops/bubbles. *J. Fluid Mech.* **160**, 511–529.

SIDEMAN, S. & GAT, Y. 1966 Direct contact heat transfer with change of phase: spray-column studies of a three-phase heat-exchanger. *AIChE J.* **12**, 296–303.

SIDEMAN, S. & HIRSCH, G. 1965 Direct contact heat transfer with change of phase: condensation of single vapor bubbles in an immiscible liquid medium. Preliminary studies. *AIChE J.* **11**, 1019–1025.

SIDEMAN, S., HIRSCH, G. & GAT, Y. 1965 Direct contact heat transfer with change of phase: effect of the initial drop size in a three-phase heat-exchanger. *AIChE J.* **11**, 1081–1087.

TOCHITANI, Y., MORI, Y. H. & KOMOTORI, K. 1977*a* Vaporization of single drops in an immiscible liquid. Part I. Forms and motions of vaporizing drops. *Wärme Stoffübertrag.* **10**, 51–59.

TOCHITANI, Y., NAKAGAWA, T., MORI, Y. H. & KOMOTORI, K. 1977*b* Vaporization of single liquid drops in a immiscible liquid. Part II. Heat transfer characteristics. *Wärme Stoffübertrag.* **10**, 71–79.

TORZA, S. & MASON, S. F. 1970 Three phase interaction in shear and electrical fields. *J. Colloid Interface Sci.* **33**, 67–83.

VUONG, S. T. & SADHAL, S. S. 1989 Growth and translation of a liquid–vapour compound drop in a second liquid. Part 2. Heat transfer. *J. Fluid Mech.* **209**, 639–660.